

# Timing Jitter and Pump-Induced Amplitude Modulation in the Colliding-Pulse Mode-Locked (CPM) Laser

George T. Harvey, *Member, IEEE*, Michael S. Heutmaker, Peter R. Smith, Martin C. Nuss, Ursula Keller, and Janis A. Valdmanis

**Abstract**—We characterize the timing jitter and spurious amplitude modulation of colliding-pulse mode-locked (CPM) lasers. The absolute jitter (the jitter of the laser alone) varied between 5 and 10 ps rms in a 50 to 500 Hz bandwidth. The smallest measured relative jitter (timing fluctuations between the CPM and a radio-frequency (RF) synthesizer synchronized to the CPM) was 1.8 ps rms in a 2 Hz to 1 kHz bandwidth. Separate from the jitter, spurious modulation in the CW pump laser mixes with the CPM pulse train to produce a set of discrete amplitude-modulated sidebands in the power spectrum of the CPM output. The frequencies of these sidebands change with cavity length, and the sidebands can be eliminated by operating the pump laser in a single longitudinal mode.

## I. INTRODUCTION

THE colliding-pulse mode-locked (CPM) laser [1], [2] is a stable source of subpicosecond pulses that are used in many studies of ultrafast phenomena. Understanding the noise characteristics of the CPM is critical for experiments that require both high temporal resolution and high sensitivity. The timing jitter of the laser can degrade the temporal resolution of electrooptic sampling techniques [3], [4] while amplitude noise limits the ability of the experiment to achieve shot-noise-limited sensitivity.

In electrooptic sampling, the temporal resolution depends on both the duration of the optical pulse and the timing jitter [5], [6] between the optical pulse train and the electrical signal of interest. Since the CPM is passively mode locked, it is convenient to use the laser as the master oscillator of the electrooptic sampling system, and to lock electrical signals to the CPM repetition rate. (Although it seems feasible to phase lock the CPM to an external 100 MHz clock, we did not try this configuration.) In this work we calculate the absolute and relative timing jitter of the CPM from frequency domain measurements of the phase noise. We refer to the timing jitter of the CPM alone as absolute jitter, and we refer to the jitter between the CPM and a phase-locked RF synthesizer as relative jitter. In electrooptic sampling, the relative timing jitter between the optical pulses and the electrical signal must be minimized for optimum time resolution. Locking the electrical signal to the CPM improves timing resolution by reducing the relative jitter to a point well under the intrinsic absolute jitter of the CPM.

Manuscript received March 12, 1990; revised September 28, 1990.

G. T. Harvey and M. S. Heutmaker are with AT&T Bell Laboratories, Princeton, NJ 08540.

P. R. Smith is with AT&T Bell Laboratories, Murray Hill, NJ.

M. C. Nuss and U. Keller are with AT&T Bell Laboratories, Holmdel, NJ.

J. A. Valdmanis is with the University of Michigan, Ann Arbor, MI 48109.

IEEE Log Number 9041874.

Previous measurements on absolute jitter by von der Linde reported less than 50 fs of jitter [7] in the CPM. These measurements, however, only looked at frequency offsets exceeding a few kHz [8]. The 5 to 10 ps jitter we measured was noticeable only at lower frequencies in the range of 50 to 500 Hz. In this frequency range, similar jitter is also seen in von der Linde's laser [8].

Spurious amplitude-noise sidebands have previously been reported in the literature [7]. We have found that these sidebands are the result of the interaction of the pump laser with the CPM. The CPM is pumped by a CW argon ion laser, which contains a small amount of spurious modulation at harmonics of its cavity round-trip frequency, caused by longitudinal mode beating. The mixing of the spurious-pump modulation with the CPM pulse train produces a set of discrete noisy sidebands in the CPM output which can be eliminated by operating the pump laser in a single longitudinal mode.

## II. EXPERIMENTAL METHOD

The cavity of the balanced CPM laser [2] is shown in Fig. 1, where the gain medium is Rhodamine-6G, and the saturable absorber is DODCI. The pump laser is a Coherent Innova 200 argon ion laser, operated at 3.0 W average power in the 514.5 nm line. The CPM produces two output beams of 620 nm wavelength at an average power of 25 mW per beam. The pulse repetition frequency is 100 MHz and the pulsewidth is on the order of 100 fs.

The absolute phase noise and the amplitude noise of the CPM are characterized in the frequency domain with a microwave spectrum analyzer (HP 8566) [5]–[9]. The input to the spectrum analyzer is a GaAs photoconductive switch with a risetime of ~5 ps and a pulsewidth of ~70 ps FWHM. The output of the switch is amplified by a 18 GHz bandwidth amplifier with 35 dB of gain.

In order to measure the relative phase noise between the CPM and an external synthesizer, a homodyne configuration with a phase detector [10] is used. Fig. 2 shows the experimental configuration. The divider generates a 10 MHz square wave from the 100 MHz output of a photodetector monitoring the laser pulses. This 10 MHz signal is used as an external reference for a radio frequency (RF) or microwave synthesizer. To test the synchronization between the synthesizer and the laser, part of the detector output is attenuated, band-pass filtered, and combined with a 100 MHz signal from the synthesizer in a double-balanced mixer. Amplitude-to-phase modulation (AM-PM) conversion [5] can occur in either the band-pass filter or the mixer if the signal levels in these components are high enough

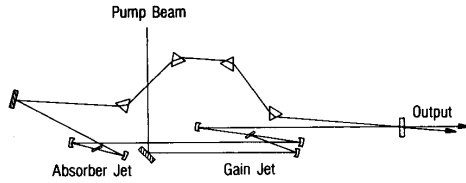


Fig. 1. The cavity of the balanced CPM laser.

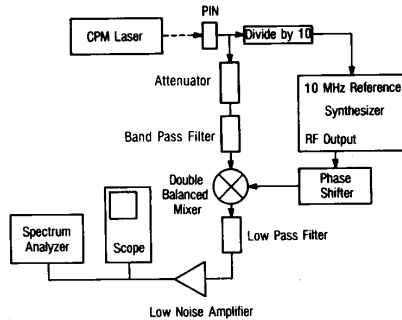


Fig. 2. Experimental configuration for measurement of the relative phase noise.

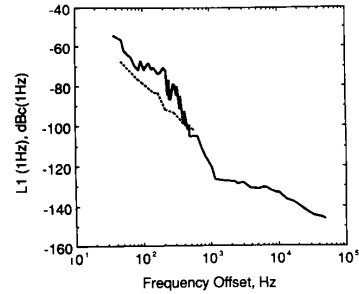
to cause nonlinear operation. By offsetting the synthesizer frequency and reducing the photodiode signal to a level that eliminates harmonics of the beat frequency, we obtain linear operation. A low-pass filter eliminates the high-frequency components of the mixer output, and the amplified signal is viewed on a low-frequency spectrum analyzer and an oscilloscope. For proper phase detection, the phase of the synthesizer output is adjusted so the two inputs to the mixer are in quadrature, by nulling the dc mixer output on the oscilloscope.

### III. RESULTS

The major feature of the RF power spectrum of the CPM is a series of delta functions at harmonics of 100 MHz, the pulse repetition rate of the CPM. Timing jitter and amplitude noise appear as phase and amplitude-noise sidebands convolved around each harmonic of the cavity frequency. Phase noise can be distinguished from amplitude noise by its dependence on the square of the harmonic number which makes it the dominant noise term at the higher harmonics. In addition to the harmonics at the repetition rate, a series of discrete sidebands appear in the power spectrum due to interactions between the modes of the CPM and the pump laser.

#### A. Timing Jitter

**Absolute Jitter:** The basic measurement of timing stability is the single-sideband phase noise density at the first harmonic  $L_1(f)$  which is expressed in dB below the carrier power (dBc) in a 1 Hz bandwidth at a frequency offset  $f$  from the carrier [5], [6], [7], [9]. Phase noise is calculated by measuring the noise spectrum of the laser at a harmonic high enough for the phase-noise sidebands to dominate over the amplitude-noise sidebands in the spectrum [5]–[7], [9]. The measurement on the spectrum analyzer must be divided by the equivalent noise bandwidth (ENBW) to obtain  $L_n(f)$ , the phase noise at the  $n$ th harmonic

Fig. 3. Two plots of  $L_1(f)$  of the CPM laser.

in a 1 Hz bandwidth. Dividing  $L_n(f)$  by  $n$  squared translates the phase noise to the fundamental frequency giving  $L_1(f)$ . The relationship between the rms phase noise  $\phi_{\text{rms}}$  and the phase-noise spectral density  $L_1(f)$  can be derived from [9];

$$\phi_{\text{rms}} = \sqrt{2 \int_{f=1/4\Delta T}^{f_{\text{upper}}} L_1(f) df} \quad (1)$$

where  $\phi_{\text{rms}}$  represents the rms phase jitter of the laser pulse over the measurement time  $\Delta T$ . The laser repetition rate  $f_i$  determines the upper frequency limit  $f_{\text{upper}}$ . The rms timing jitter  $t_{\text{rms}}$  is equal to  $\phi_{\text{rms}}/2\pi f_i$ .

We have measured the absolute jitter on two different CPM lasers of the same balanced cavity design. Fig. 3 shows two measurements of  $L_1(f)$ . The dashed line represents typical jitter from a well-running laser and indicates an rms jitter of 5 ps (3.5 millirad) in the frequency span between 50 and 500 Hz. The solid line, which was taken to extend the frequency range of the measurement, was also taken the day after a dye change and indicates a jitter of 10 ps (7 mrad) over the same 50 to 500 Hz range. The increased jitter comes mainly from increased noise at frequencies between 100 and 400 Hz and may be due to a larger number of bubbles in the dye.

For low frequency offsets we measure noise at the 10th harmonic of the laser repetition rate where phase noise dominates amplitude noise out to about 500 Hz. Above 500 Hz, the 100th harmonic was used for measurement.

The phase noise drops off rapidly at a rate of 30 to 40 dB per decade out to a frequency of 1 kHz. At such a sharp roll off, there is little contribution to the jitter due to frequencies higher than twice the lower frequency used in the integration. Even after the roll off decreases to 10 dB per decade at 1 kHz, the contribution to the jitter due to frequencies greater than 1 kHz can be neglected. Since the phase noise is predominantly at lower frequencies, it should be feasible to reduce the jitter by actively controlling the cavity length and phase locking the frequency of the laser to a stable frequency source.

The absolute timing jitter depends critically on measurement time. The 5 to 10 ps jitter found above 50 Hz corresponds to a measurement time of 5 ms. As the measurement time is increased, the jitter goes up dramatically. If  $L_1(f)$  is integrated down to a frequency of 37 Hz on the solid curve in Fig. 3, a measurement time of 7 ms, the timing jitter jumps from 10 to 17.5 ps.

The measured absolute timing jitter is consistent with sub-micron variations in cavity length occurring in the frequency range of 50–500 Hz. A small and slow change in cavity length leads to significant variation in the phase of the laser pulse train

because the phase change accumulates over many round-trip times of the cavity. Periodic changes in cavity length  $L$ , at a frequency  $f_m$  modulate the laser cavity frequency  $f_l$ . For small differences in cavity length, the maximum frequency deviation  $\delta f_l$  is related to the maximum change in cavity length  $\delta L$  by

$$\frac{\delta f_l}{f_l} = \frac{\delta L}{L}. \quad (2)$$

If  $\delta f_l \ll f_l$ , the corresponding phase modulation  $\delta \phi = \delta f_l / f_m$ , and

$$\delta \phi = \frac{\delta L}{L} = \frac{f_l}{f_m}. \quad (3)$$

To find the maximum timing variation of the pulse  $\delta t$  we substitute  $\delta \phi = 2\pi f_l \delta t$  into (3) and solve for  $\delta t$ , which yields

$$\delta t = \frac{\delta L}{2\pi L f_m}. \quad (4)$$

To get an estimate of the sensitivity of the timing jitter to cavity length changes, we calculate  $0.01 \mu\text{m}$  as the cavity length change required at a modulation frequency of 100 Hz to cause a 5 ps timing jitter in the laser. Although this example uses a discrete frequency when, in reality, the cavity length changes are distributed over the entire frequency range, it is clear that substantial jitter can result from extremely small low-frequency changes in cavity length.

We tried several experiments to try to isolate the source of the jitter that were inconclusive. Although the dye jet seems a likely candidate for causing the jitter, moving the collection tube to change the stability of the jet did not significantly alter the jitter. Likewise, changing the pulsewidth by tuning the prisms in the laser had no effect.

We were able to induce jitter acoustically by driving the laser enclosure with a loudspeaker. At a frequency of 340 Hz (one of the resonance frequencies of the enclosure for the CPM), the acoustic modulation produces phase-noise sidebands in the CPM output, as shown in Fig. 4. At the tenth harmonic (the upper trace in Fig. 4), the first-order sidebands are enhanced by 20 dB compared with those on the fundamental (the lower trace), as expected for phase modulation. For acoustic frequencies above about 400 Hz, the first-order modulation sidebands do not increase as  $n^2$  with harmonic number, which indicates the presence of both phase and amplitude modulation.

Using (1) the phase modulation due to the acoustic noise is 11 mrad rms which corresponds to a cavity length modulation of  $0.11 \mu\text{m}$  calculated using (3). Although it might seem plausible that ambient acoustic noise from the room might be vibrating the laser enclosure, dampening the interior of the enclosure with acoustic absorbers did not alter the jitter. Also, the spectrum of the phase noise did not show any structure that might be expected from the discrete acoustic modes of the enclosure.

Further investigation is needed to pinpoint the exact source of the laser jitter. Vibration of the cavity mirrors or the dye jet are likely causes of the jitter but the source of the noise and how it is coupled to the elements in the cavity are currently unknown.

**Relative Jitter:** The relative timing jitter is calculated from the relative phase noise shown in Fig. 5. The upper trace shows the relative phase noise from 1 to 100 Hz, using a Programmed Test Sources (PTS) Model 160 synthesizer synchronized with the CPM. The lower trace shows the noise floor of the phase detection system when the CPM beam is blocked.

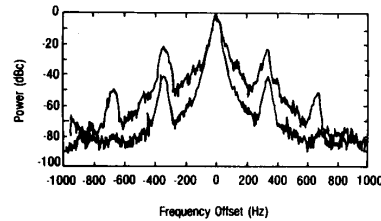


Fig. 4. Relative phase noise sideband (upper trace) and noise floor of measurement system (lower trace).

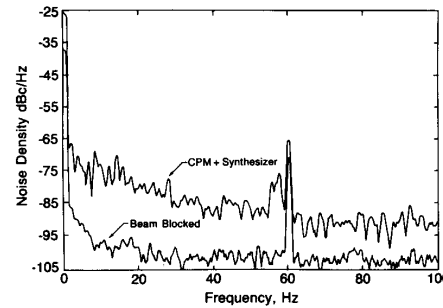


Fig. 5. Power spectrum of the fundamental and the tenth harmonic in the presence of acoustic modulation of the CPM cavity.

The method for determining the relative timing jitter is similar to the method discussed for absolute timing jitter. To find the single-sideband phase-noise density  $L_1(f)$  the power-spectral density is divided by four times the carrier power. The factor of four accounts for the folding of the lower sideband into the upper sideband around 0 Hz as a result of the mixing [10]. The timing jitter is derived from  $L_1(f)$  using (1). Discrete spurious signals, such as the signal at 60 Hz in Fig. 5, are excluded from the integration of the phase noise.

Of the three synthesizers we tested with the CPM, the PTS synthesizer has the lowest relative phase noise, 1.1 millirad rms over a 2 Hz to 1 kHz band. This phase jitter corresponds to an rms timing jitter of 1.8 ps for a 0.125 s measurement time. The maximum output frequency of the PTS-160 is 160 MHz. The relative jitter depends on the characteristics of the synthesizer, and it is significantly greater for two other synthesizers with higher maximum output frequencies. Over the same frequency band, the relative jitter is 5 ps rms using the Hewlett-Packard 8660C synthesizer (maximum frequency 2.6 GHz) and it is 6 ps rms using the HP 8673D (maximum frequency 26 GHz).

When the CPM is the master oscillator in the system, several possible sources of relative jitter can be identified. Any residual jitter (jitter introduced by the synthesizer in the creation of new frequencies) will appear as relative jitter. From 10 Hz to 1 kHz (the range where specifications can be compared to data), the relative phase noise using both the PTS160 and the HP 8660C is at least 10 dB above the absolute phase noise specifications of the instruments. The smaller instrument specification indicates that the relative jitter is not dominated by jitter due to the synthesis process in these instruments. In the HP 8673D, the specified absolute jitter of the synthesizer is more than the measured relative jitter and the jitter in the synthesis process could be contributing to the jitter between the laser and the synthesizer.

Another source of relative jitter is amplitude-to-phase modulation (AM-PM) conversion in the interaction between the signal from the photodiode and the divider circuit (or at the synthesizer input if the synthesizer can use a 100 MHz reference). Jitter due to the divider must be equal to or less than the lowest measured jitter of 1.8 ps in the PTS 160. The 5 ps jitter in the HP 8660C must be dominated by other sources.

The absolute jitter of the CPM produces phase variations in the time base of the synthesizer, and the ability of the synthesizer to track these variations will affect the relative jitter. The PTS synthesizes its output directly from the external frequency source, which is first filtered by a crystal filter with a 250 Hz bandwidth. The translated bandwidth at 100 MHz is 2.5 kHz which allows the synthesizer to track the low-frequency noise that dominates the absolute jitter of the laser. Both HP synthesizers use a phase-locked loop at the external source input. The loop bandwidth, which is not specified, could be limiting the ability of the synthesizers to track the laser jitter.

### B. Pump-Induced Spurious Sidebands

As seen in Fig. 6(a), the spectrum of the CPM laser contains a series of spurious sidebands convolved around the fundamental cavity frequency and its harmonics. We attribute these sidebands to mixing of the longitudinal modes of the argon pump laser with the cavity modes of the CPM. The new frequencies resulting from the mixing process occur at the sum and difference frequencies of the two sets of cavity modes. Since the mixing is due to output power fluctuations in the pump laser modulating the gain in the CPM laser without substantially changing the frequency of the CPM cavity, the modulation is expected to be amplitude and not phase modulation. Indeed, our experiments show that the power in these sidebands is independent of harmonic number, which indicates amplitude modulation.

We confirm the origin of the spurious sidebands by inserting an etalon into the pump laser cavity, which forces it to operate in a single longitudinal mode. In single-mode operation, the argon laser no longer has frequency components at multiples of the cavity frequency; mixing no longer occurs in the CPM gain jet; and the sidebands are absent. Fig. 6(b) shows the CPM spectrum when the pump laser is in single-mode operation, and the spurious sidebands are absent. The deletion of the sidebands has no effect on the phase noise in the CPM laser, which is not altered by insertion of the etalon.

The sideband frequencies are directly related to the ratio of the two laser cavity lengths. When the cavity frequency of the pump laser is a rational fraction of the cavity frequency of the CPM, some of the mixing products overlap, which reduces the number of sidebands in the spectrum. Fig. 6(a) is a spectrum where the CPM cavity length is 16/21 of the argon cavity length. This spectrum contains 20 evenly spaced sidebands between each harmonic of the CPM cavity frequency. In general, the number of sidebands will be one less than the denominator of the cavity length ratio, as shown in the Appendix.

As  $L$  varies and the two cavity frequencies are no longer in the original rational ratio, a larger number of distinct mixing frequencies is possible, and each mixing product produces a peak in the spectrum. The result of this effect is that the distribution of spurious peaks in the spectrum changes dramatically with CPM cavity length, as shown in Fig. 7. Fig. 7(a) contains the same spectrum as in Fig. 6(a), expanded to show just a few of the regularly spaced sidebands. Each of these main sidebands

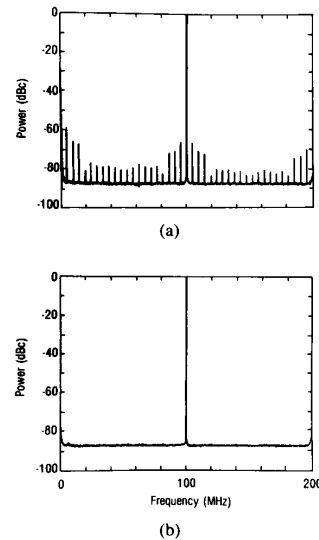


Fig. 6. (a) RF spectrum showing spurious sidebands between the harmonics of the cavity frequency. (b) RF spectrum showing the elimination of the spurious sidebands by running the pump laser in a single longitudinal mode.

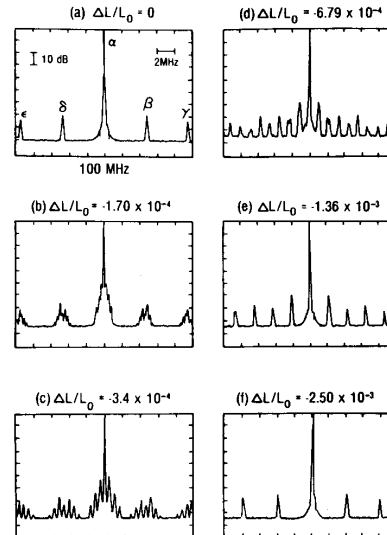


Fig. 7. RF spectra showing the evolution of the main sidebands into subsidiary peaks as the CPM cavity length is varied.

is denoted by a letter:  $\alpha$ ,  $\beta$ ,  $\gamma$ ,  $\delta$ , and  $\epsilon$ . As the cavity length is decreased each of the main sidebands splits into a number of subsidiary peaks [Fig. 7(b) and (c)]. These new peaks travel in both directions in frequency away from the original peak, which moves relatively slowly. The sets of peaks overlap to various degrees [Fig. 7(d) and (e)] as cavity length is decreased further, and eventually form a new set of main sidebands with a different spacing [Fig. 7(f)]. The fractional CPM cavity length change  $\Delta L/L_0$  is shown in each spectrum in Fig. 7.

The frequencies of the sidebands exactly match the mixing products calculated using the cavity frequencies of the pump

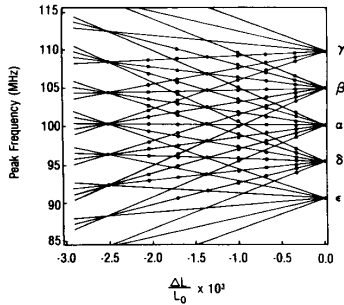


Fig. 8. Frequencies of the subsidiary peaks as a function of CPM cavity length. The solid lines are calculated mixing frequencies between the CPM pulse train and the spurious pulses of the pump laser.

laser and the CPM. The points in Fig. 8 show the measured peak frequencies as a function of  $\Delta L/L_0$  for a set of spectra including those of Fig. 7. The solid lines are calculated mixing frequencies, and each line indicates the frequency of an individual peak as the cavity length varies. (The calculation of the mixing frequencies is explained in the Appendix.) Thus, each set of lines fans out from  $\Delta L/L_0 = 0$ , where the subsidiary peaks overlap to form the main sidebands, and the labels on the right-hand vertical axis correspond to those in Fig. 7(a).

As  $L$  varies over the range shown in Fig. 8, the subsidiary peaks overlap significantly at two different cavity lengths, and we can calculate the cavity frequency ratio for these conditions. When  $\Delta L/L_0 = -0.00136$ , then the new cavity ratio is  $\frac{16}{21}$  ( $1 - 0.00136$ )  $\approx \frac{35}{46}$  where  $\frac{16}{21}$  is the original cavity ratio. For the new cavity length, we find that the CPM spectrum contains 45 sidebands between harmonics, as expected. Similarly, when  $\Delta L/L_0 = -0.0025$ , the new ratio is  $\approx \frac{19}{25}$  and the spectrum contains 24 sidebands. Portions of these two spectra are shown in Fig. 7(e) and (f).

We have observed the RF spectrum of the argon ion pump laser, and find spurious modulation at the cavity frequency (76 MHz) and harmonics, due to longitudinal-mode beating. The fractional modulation of the pump beam power is on the order of 0.004. If the same modulation depth was present on the CPM output, the modulation products would be suppressed on the order of 50 dB (electrical) on the spectrum analyzer. In fact the suppression of the sidebands varies from 60 to 80 dB, but the above estimate does not account for losses or nonlinearities in the mixing process. Also, the spectral peaks are not sharp, but have a typical 3-dB (electrical) full width of 170 kHz. Thus, the coherence time of the spurious pump pulses is on the order of 6  $\mu$ s.

The spectrum of the spurious amplitude modulation of the CPM provides indirect information about the number of longitudinal modes in the pump laser. As shown in the Appendix, in order to produce the observed six subsidiary peaks from each main sideband, the pump laser spectrum must contain power out to about the 60th harmonic of its cavity frequency, i.e., contain  $\sim 60$  longitudinal modes within its gain bandwidth. This is consistent with the 8 GHz bandwidth of the argon laser line at 514 nm.

In the measurement of a small signal on the CPM beam, experimental sensitivity is degraded if one of the spurious sidebands lies within the passband of the detection system. In some cases a narrow-band detection system could be positioned in a part of the spectrum in between the spurious sidebands. In the

balanced CPM laser, however, the pulsewidth is optimized by tuning the group dispersion by altering the path length through one of the prisms. Changing the path length alters the CPM cavity frequency, changing the frequencies of the spurious sidebands. To prevent excess laser noise from affecting the measurement, the sidebands must be either constantly monitored or eliminated entirely by running the pump laser in a single longitudinal mode.

#### IV. CONCLUSION

We observe absolute jitter of 5 to 10 ps rms at 100 MHz (over a frequency range of 50–500 Hz), for a CPM laser on two different lasers of the same cavity design. Small changes in effective cavity length on the order of 0.01  $\mu$ m would account for the jitter. At this time the origins of the cavity length changes are only speculative.

In electrooptic sampling, the signal driving the device can be phase locked to the frequency of the laser cavity. In this configuration, degradation in temporal resolution depends on the relative timing jitter between the laser pulses and the electrical signal, and not the absolute jitter of the laser. In our experiments where we locked several different synthesizers to the laser, we measure between 1.8 and 6 ps rms relative timing jitter over a frequency range of 2 Hz to 1 kHz. The amount of relative jitter depends on the characteristics of the RF synthesizer that is synchronized to the CPM.

The amplitude noise spectrum of the CPM laser is sensitive to contributions from the mixing of longitudinal modes of the Argon ion pump laser with the CPM pulse train. This mixing produces a series of discrete sidebands that shift in frequency as the cavity length of the CPM is changed. The excess noise of the sidebands reduces detection sensitivity in many experiments. These sidebands can be removed by operating the pump laser in a single longitudinal mode. Spurious sidebands have also recently been observed on a passively mode-locked color center laser pumped by a multimode CW Nd:YAG laser [11]. In general, multimode laser pumps can be expected to generate spurious sidebands on most passively mode-locked lasers.

#### APPENDIX

##### CALCULATION OF MIXING FREQUENCIES

First we show that when the cavity frequencies of the pump laser and the CPM laser are in a rational ratio, the denominator of the ratio determines the number of main sidebands between the CPM harmonics, as in the spectrum of Fig. 6(a). If the cavity frequency of the CPM is  $f_{\text{CPM}} = f_0$  and that of the pump laser is  $f_{\text{pump}} = m/n f_{\text{CPM}}$ , then the difference frequency is

$$f_{\text{mix}} = \left| f_0 - \frac{m}{n} f_0 \right| \quad (\text{A.1})$$

where  $m$  and  $n$  are integers. Since both the CPM spectrum and the pump laser spectrum have high harmonic content, the difference frequencies between harmonics are also relevant. The difference between the  $J$ th harmonic of the CPM and the  $K$ th harmonic of the pump laser is

$$f_{J,K} = \left| J - K \frac{m}{n} \right| f_0. \quad (\text{A.2})$$

Many different pairs of  $J$  and  $K$  values can be chosen to yield a given value of  $f_{J,K}$ , and it is not possible to determine from the spectrum of Fig. 6(a) how many different harmonic pairs con-

TABLE I

$\alpha: f_{J,K} = f_0  J - K \frac{16}{21}  = f_0$			$\beta: f_{J,K} = f_0  J - K \frac{16}{21}  = \frac{22}{21} f_0$		
$J$	$K$	Slope	$J$	$K$	Slope
1	0	-1	2	4	2
15	21	15	14	17	-14
17	21	-17	18	25	18
31	42	31	30	38	-30
33	42	-33	34	46	34
47	63	47	46	59	-46
49	63	-49	50	67	50

tribute to the formation of each main sideband. The number of main sidebands present in the spectrum can be understood by writing (A.2) as

$$f_{J,K} = \frac{f_0}{n} |nJ - mK|. \quad (\text{A.3})$$

It is clear that the smallest possible difference between mixing products is  $\Delta f_{J,K} = f_0/n$ , since the quantity  $nJ - mK$  will always be an integer. The number of sidebands in each frequency interval of size  $f_0$  is given by

$$N = \frac{f_0}{\Delta f_{J,K}} - 1 = n - 1. \quad (\text{A.4})$$

Thus for the spectrum of Fig. 6(a) the denominator  $n = 21$ , since the number of sidebands between adjacent CPM harmonics is  $N = 20$ .

The splitting of the sidebands shown in Fig. 7 occurs when the variation of  $f_{\text{CPM}}$  causes the difference frequency  $f_{J,K}$  to change. As  $L$  changes, the cavity frequency of the CPM is

$$f_{\text{CPM}} \approx f_0 \left(1 - \frac{\Delta L}{L_0}\right) \quad (\text{A.5})$$

for small  $\Delta L/L_0$ . Then the difference of the  $J$ th harmonic of the CPM and the  $K$ th harmonic of the pump laser is

$$f_{J,K} = f_0 \left| J \left(1 - \frac{\Delta L}{L_0}\right) - K \frac{m}{n} \right| \quad (\text{A.6})$$

and the value of  $J$  determines the variation of  $f_{J,K}$  with  $\Delta L$ .

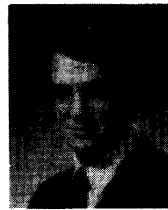
We use (A.6) to calculate the frequencies of the subsidiary peaks, and to match the data of Fig. 8, in the following way. Since  $f_{\text{pump}} \approx 76$  MHz and  $n = 21$ , the most likely value for the initial cavity frequency ratio  $m/n$  is  $16/21 \approx 0.7619$ . For each main sideband of Fig. 7(a) we use (A.1) to find pairs of values  $J$  and  $K$  that yield the main sideband frequency, as shown in Table I for the  $\alpha$  and  $\beta$  sidebands. When  $\Delta L = 0$ , many  $J, K$  values yield the same mixing frequency; for example,  $f_{J,K} = f_0$  for the  $\alpha$  sideband and  $f_{J,K} = \frac{22}{21} f_0$  for the  $\beta$  sideband. For nonzero  $\Delta L$ , each frequency  $f_{J,K}$  becomes distinct, and the magnitude of the slope of  $f_{J,K}$  versus  $\Delta L/L_0$  is  $J$ , as shown in (A.6). The sign of the slope is determined by the absolute value function in (A.6). If  $J f_{\text{CPM}} > K f_{\text{pump}}$  the slope is  $-J$ , otherwise the slope is  $+J$ ; the appropriate value is shown in Table I. The solid lines in Fig. 8 show the values of  $f_{J,K}$  versus  $\Delta L/L_0$  calculated from (A.6) using  $J$  and  $K$  values such as in Table I. The agreement between the data points and the calculated mixing frequencies is excellent.

## ACKNOWLEDGMENT

We acknowledge useful discussions with J. M. Wiesenfeld and M. J. W. Rodwell.

## REFERENCES

- [1] R. L. Fork, B. I. Greene, and C. V. Shank, "Generation of optical pulses shorter than 0.1 ps by colliding pulse mode locking," *Appl. Phys. Lett.*, vol. 38, p. 671, 1981.
- [2] J. A. Valdmanis and R. L. Fork, "Design considerations for a femtosecond pulse laser balancing self phase modulation, group velocity dispersion, saturable absorption, and saturable gain," *IEEE J. Quantum Electron.*, vol. 22, p. 112, 1986.
- [3] J. A. Valdmanis, "1-THz bandwidth probe for high-speed devices and integrated circuits," *Electron. Lett.*, vol. 23, p. 1308, 1987.
- [4] B. H. Kolner and D. M. Bloom, "Electrooptic sampling in GaAs integrated circuits," *IEEE J. Quantum Electron.*, vol. 22, p. 79, 1986.
- [5] M. J. W. Rodwell, D. M. Bloom, and K. J. Weingarten, "Subpicosecond laser timing stabilization," *IEEE J. Quantum Electron.*, vol. 25, p. 817, 1989.
- [6] J. Kluge, D. Wiechert, and D. von der Linde, "Fluctuations in synchronously mode-locked dye lasers," *Opt. Commun.*, vol. 51, p. 201, 1986.
- [7] D. von der Linde, "Characterization of the noise in continuously operating mode-locked lasers," *Appl. Phys. B*, vol. 39, p. 201, 1986.
- [8] D. von der Linde, personal communication.
- [9] U. Keller, K. D. Li, M. Rodwell, and D. M. Bloom, "Noise characteristics of femtosecond fiber Raman soliton lasers," *IEEE J. Quantum Electron.*, vol. 25, p. 280, 1989.
- [10] Hewlett-Packard Product Note 11729B-1, "Phase Noise Characterization of Microwave Oscillators: Phase Detector Method," 1984.
- [11] U. Keller, C. E. Soccolich, G. Sucha, M. N. Islam, and M. Wegener, "Noise characteristics of femtosecond color center lasers," *Opt. Lett.*, to be published.



**George T. Harvey** (M'81) was born in Baltimore, MD, in 1949. He received the B.S. degree in electrical engineering from Lehigh University, Bethlehem, PA, in 1974 and the Ph.D. degree in optics from the University of Rochester, Rochester, NY, in 1980.

Since 1980, he has been a member of the technical staff with the Engineering Research Center, AT&T Bell Laboratories, Princeton, NJ. His current research involves short pulse laser systems and optical probing of high-speed

integrated circuits.

Dr. Harvey is a member of the Optical Society of America.

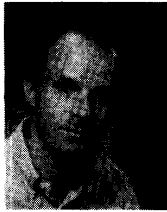


**Michael S. Heutmaker** was born in Minneapolis, MN, in 1958. He received the B.S. degree in physics from Washington University, St. Louis, MO, in 1980 and the Ph.D. degree in physics from the University of Pennsylvania, Philadelphia, in 1986.

He has been a member of the technical staff with AT&T Bell Laboratories, Princeton, NJ, since 1986, and has been working on optical probing of high-speed circuits.

**Peter R. Smith** grew up in the Bronx, NY. He received the B.S.E.E. degree in 1972 from Northeastern University, Boston, MA. In 1975 he received the M.S.(E.E.) degree and the Electrical Engineer (professional) degree in 1977, both from Columbia University, New York, NY.

He is currently a member of the technical staff with the Heterostructure Electronics Research Department, AT&T Bell Laboratories, Murray Hill, NJ. Prior to this position he spent 11 years with the High Speed Materials and Phenomena Research Department developing optoelectronic measurement techniques with picosecond time resolution. His present research interests include the application of these high-speed measurement techniques to the characterization and modeling of fast devices and circuits.



**Martin C. Nuss** was born in Lörrach, West Germany, in 1957. He received the Vordiplom in physics from the University Freiburg in 1978 and the Diplom and the Ph.D. degree in physics in 1982 and 1985, respectively, both from the Technical University, Munich, West Germany, where he has been involved in ultrafast spectroscopy of semiconductors, molecular dynamics, and primary processes in photosynthesis.

He joined AT&T Bell Laboratories, Murray Hill, NJ, in 1985 as a postdoctoral fellow, and has been a member of the technical staff in the Quantum Physics and Electronics Research Department in Holmdel, NJ, since 1987. His research activities include ultrafast optoelectronics and spectroscopy. His current interest focuses on high-speed electron transport in semiconductors and on far-infrared properties of high- $T_c$  superconductors.

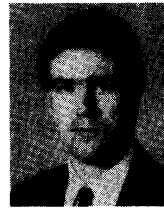
Dr. Nuss is a member of the Optical Society of America and the American Physical Society.



**Ursula Keller** was born on June 21, 1959 in Zug, Switzerland. She received the Diplom in experimental physics from the Federal Institute of Technology (ETH) Zurich, Switzerland in 1984 and the M.S. and Ph.D. degrees in applied physics from Stanford University, Stanford, CA, in 1987 and 1989, respectively. From late 1984 to 1985 she had a research fellowship to work on optical bistability at Heriot-Watt University, Edinburgh, Scotland with Prof. S. D. Smith. Her Ph.D. research was in the optical probing of charge and voltage in GaAs integrated circuits with Prof.

D. M. Bloom.

Since 1989 she has been employed as a member of the technical staff of AT&T Bell Laboratories, Holmdel, NJ, where she conducts research on photonic switching and short pulse laser research. During 1985-1986 she was a Fulbright Fellow and in 1987-1988 she received an IBM Predoctoral Fellowship.



**Janis A. Valdmanis** was born in Old Windsor, England, in 1956 and emigrated to the United States in 1967. He received the B.S. degrees in physics and mathematics from Purdue University, West Lafayette, IN, in 1978 and the Ph.D. degree in optics from the University of Rochester, Institute of Optics, Rochester, NY, in association with the University's Laboratory for Laser Energetics in 1983.

From 1983 to 1988, he was a member of the technical staff of AT&T Bell Laboratories, Murray Hill, NJ. In September 1988, he moved to the University of Michigan, Ann Arbor, as an associate professor of optics in the Department of Electrical Engineering and Computer Science. He is also the associate director of the Ultrafast Science Laboratory. His current research interests are focused on femtosecond laser systems and ultrafast optoelectronic instrumentation.

Dr. Valdmanis is a Fellow of the Optical Society of America (1990), and in 1988 he received the Society's Adolph Lomb Medal for his contributions to ultrafast optical instrumentation.